Alumina-Supported Vanadium Nanoparticles: Structural Characterization and CO Adsorption Properties

Norbert Magg, Javier B. Giorgi,[†] Martin M. Frank,[‡] Boonchuan Immaraporn, Thomas Schroeder,[§] Marcus Bäumer,[||] and Hans-Joachim Freund*

Contribution from the Fritz-Haber-Institut der Max-Planck-Gesellschaft, Faradayweg 4-6, 14195 Berlin, Germany

Received October 28, 2003; E-mail: freund@fhi-berlin.mpg.de

Abstract: Alumina-supported vanadium particles were prepared under ultrahigh vacuum (UHV) conditions and characterized with respect to their structural and CO adsorption properties. As supporting oxide, we used a thin, well-ordered alumina film grown on NiAl(110). This allows the application of scanning tunneling microscopy (STM), infrared reflection−absorption spectroscopy (IRAS), and X-ray photoelectron spectroscopy (XPS) without charging effects. Vanadium evaporation under UHV conditions leads to the growth of nanometer-sized particles which strongly interact with the alumina support. At very low vanadium coverages, these particles are partially incorporated into the alumina film and get oxidized through the contact to alumina. Low-temperature CO adsorption in this coverage regime permits the preparation of isolated vanadium carbonyls, of which we have identified mono-, di-, and tricarbonyls of the $V(CO)_y$ type. A charge−frequency relationship was set up which allows one to quantify the extent of charge transfer from vanadium to alumina. It turns out that this charge transfer depends on the V nucleation site.

1. Introduction

Because of its importance in technical applications such as thin film technology, electronic devices, gas sensors, and heterogeneous catalysis, the interaction of metals with oxide surfaces has been subject to many surface science studies dealing with the metal−oxide interface region.[1,2] Among the various systems examined in the past, frequently by X-ray photoelectron spectroscopy (XPS), the $TiO_2(110)$ surface represents one of the most thoroughly investigated substrates. It was shown that oxidation/reduction reactions take place at the metal−titania interface, whose extent correlates with the reactivity of the overlayer toward oxygen.[3] For V on titania, annealing in ultrahigh vacuum (UHV) even allowed one to grow locally ordered VO_x ($x \approx 1$) films of up to 5 ML thickness.[4] That titania can easily be reduced appears to be an important factor.

The situation is more complex for oxides such as Al_2O_3 which adopt only a single stable oxidation state. In addition, metal−alumina interactions seem to depend strongly on preparative issues which affect the densities and types of alumina surface defects, the presence of OH groups, and the nature of the surface termination. For metal-backed oxide films, even the rigidity of the underlying metal might play a decisive role for metal adhesion.[5] Hence, a conclusive picture has not been established so far, although there is evidence that interface reactions depend on the electronegativity of the metal adlayer also in the case of alumina supports. Small coverages of early transition metals such as Ti,[6,7] V,[8] Nb,[7] and Cr[9] were found to be partially oxidized. According to density functional calculations, negative charge is donated from metal to neighboring oxygen atoms.[10,11] With increasing atomic number, the extent of this charge transfer decreases, along with Pauling electronegativity, leading to diminished metal adsorption energies.[11] Besides, late transition metals might interact with Al rather than oxygen atoms. In the case of Ni deposits, for example, the formation of Ni−Al intermetallic compounds was reported,[7] while other groups claim to have observed oxidized Ni.[9] Differences in alumina surface preparation are probably at the origin of these contradictions, but macroscopic charging and charge-induced final state effects can be a serious problem in XPS studies of such large band-gap materials as well.

The purpose of the present work is two-fold. First, it intends to contribute to a better understanding of alumina-supported metal systems, supplementing XPS data with information from scanning tunneling microscopy (STM) and infrared reflection−absorption spectroscopy (IRAS). To achieve this, the alumina

[†] Present address: University of Ottawa, Ottawa, Canada.
[‡] Present address: IBM T.J. Watson Research Center, Yorktown Heights, NY.
[§] Present address: European Synchrotron Radiation Facility, Grenoble, France.
[||] Present address: Universität Bremen, Institut für Angewandte und Physikalische Chemie, Bremen, Germany.

(1) Henrich, V. E.; Cox, P. A. *The Surface Science of Metal Oxides*; Cambridge University Press: New York, 1994.
(2) Campbell, C. T. *Surf. Sci. Rep.* **1997**, *27*, 1.
(3) Diebold, U.; Pan, J.-M.; Madey, T. E. *Surf. Sci.* **1995**, *331*, 845.
(4) Negra, M. D.; Sambi, M.; Granozzi, G. *Surf. Sci.* **1999**, *436*, 227.

(5) Jennison, D. R.; Bogicevic, A. *Surf. Sci.* **2000**, *464*, 108.
(6) Chaug, Y. S.; Chou, N. J.; Kim, Y. H. *J. Vac. Sci. Technol.,A* **1987**, *5*, 1288.
(7) Ohuchi, F. S.; Kohyama, M. *J. Am. Ceram. Soc.* **1991**, *74*, 1163.
(8) Biener, J.; Bäumer, M.; Madix, R. J.; Liu, P.; Nelson, E.;Kendelewicz, T.; Brown, G., Jr. *Surf. Sci.* **2000**, *449*, 50.
(9) Ealet, B.; Gillet, E. *Surf. Sci.* **1996**, *367*, 221.
(10) Verdozzi, C.; Jennison, D. R.; Schultz, P. A.; Sears, M.P. *Phys. Rev. Lett.* **1999**, *82*, 799.
(11) Bogicevic, A.; Jennison, D. R. *Phys. Rev. Lett.* **1999**, *82*,4050.

support employed was prepared as a thin, well-ordered film to avoid charging problems. The high reproducibility of the preparation allows one to establish reliable correlations between the reactive vanadium particles discussed here and less reactive materials such as Pd, Rh, and Ir studied previously on the same support.[12,13] In addition, the adsorption of CO on the vanadium particles facilitates the generation of well-defined, uniform vanadium carbonyls. Such species play a vital role in surface organometallic chemistry, that is, in the endeavor to bridge the gap between heterogeneous and homogeneous catalysis. This approach has the potential to supplement the traditional surface science approach as described in great detail in a recent publication.[14] Second, UHV-deposited vanadium represents an important reference system for our investigations on alumina-supported vanadium oxide particles prepared via evaporation of vanadium in an oxygen ambient. Corresponding studies are discussed elsewhere.[15−17]

2. Experimental Section

All of the experiments presented in this work have been performed in a multichamber UHV system operated at a base pressure below 2×10^{-10} mbar. Sample preparation, XPS, and infrared measurements were carried out in one part of the UHV system, and acquisition of STM images was carried out in another part. The transfer between these two stages had to be done at room temperature. Consequently, all STM images were taken at this temperature, even though a variable-temperature scanning tunneling microscope (Omicron) was employed. Tunneling was performed in the constant current mode with voltages in the range from +2.3 to +3.1 V, where electrons tunnel from filled tip states into empty sample states, and currents between 0.04 and 0.1 nA. Photoelectron spectra were recorded with a concentric hemispherical analyzer (Scienta SES 200) set to a pass energy of 150 eV. A dual-anode X-ray tube served as an excitation source for Al Kα radiation. Infrared spectra were acquired with a Fourier transform infrared spectrometer (Bruker IFS 66v/S). P-polarized light was coupled into the UHV chamber via viton sealed KBr windows and reflected from the sample surface at an angle of 84°. Spectra were recorded using a liquid nitrogen cooled MCT detector operating in the mid-infrared region at frequencies above 600 cm^{-1}. Typically, 4000 scans were accumulated per spectrum. Spectral resolution after apodization was 3.3 cm^{-1}. It is important to mention that the metal surface selection rule (MSSR)[18] applies for the system discussed here. This is due to the limited thickness of the alumina film and the metal substrate underneath. Hence, only structures can be observed which exhibit a nonzero component of the dynamic dipole moment perpendicular to the NiAl substrate.

Sample preparation was carried out in two steps: the growth of the alumina film and the deposition of vanadium. The first step comprised the oxidation of a sputter-cleaned NiAl(110) surface at 550 K by exposure to about 3000 L of O$_2$ (1 L = 10^{-6} Torr s) and subsequent annealing at about 1100 K.[19] Two oxidation/annealing cycles were employed to ensure complete oxidation of the NiAl surface. This results in a well-ordered alumina film[19] of ∼5 Å thickness.[12,19,20] After the

preparation, the oxide film quality was checked by STM and LEED (low-energy electron diffraction). In a second step, vanadium (>99.8%, Goodfellow) was deposited under UHV conditions by means of an electron-beam evaporator (EFM3T, Focus). During evaporation, the sample was held on a retarding potential to prevent vanadium ions from being accelerated toward the sample. A deposition rate of 0.36 ML per min was determined by means of a quartz crystal microbalance and counterchecked by two-dimensional submonolayer growth on NiAl-(110) and subsequent STM measurements. One monolayer of vanadium (1 MLV) was defined as the interlayer distance between the close-packed (110) planes of bulk vanadium of 2.14 Å, which corresponds to 1.54×10^{15} atoms cm^{-2}.

Adsorption of CO (>99.997%, AGA) was carried out directly in the IR cell utilizing a gas-doser system (pinhole doser) and with the sample kept at about 90 K. To remove any contaminants from the CO gas feed, for example, Ni carbonyls present in the gas cylinder, the CO gas was passed through a cooling trap operated at liquid nitrogen temperature. Note that, at a sample temperature of 90 K, CO does not adsorb on the clean alumina substrate. Consequently, all CO signals observed in our IR spectra are due to the presence of vanadium.

3. Results and Discussion

Focusing on the investigation of metal−support interactions, we characterized alumina-supported vanadium particles with respect to their geometric (STM) and electronic structure (XPS) as well as to their vibrational properties (IRAS). In addition, CO molecules were utilized to probe the adsorption behavior of the system.

3.1. Structural Characterization. The results presented in this section are grouped according to the experimental techniques employed. Note, however, that there are various correlations between these subsections which can reliably be established because all measurements were performed on a single sample preparation.

3.1.1. STM Results. Figure 1 presents a series of STM images taken for increasing amounts of vanadium deposited onto the alumina film. In agreement with earlier STM studies on this system,[21] the preparation conditions (UHV, 300 K) lead to the growth of roundish, three-dimensional particles which are homogeneously distributed over the substrate surface. Typical particle diameters are in the range of 20−40 Å. Because of STM tip convolution effects, these values have to be regarded as upper limits.[12] Height information, in contrast, remains essentially unaffected by tip convolution effects but depends on the tunneling voltage applied.[12] For voltages below ca. 3 V, aluminum oxide states do not contribute to the tunneling current; that is, the NiAl surface represents the reference level for height measurements. As one is usually interested in particle heights with respect to the alumina surface, one has to correct for the alumina film thickness. The validity of this approach was proven, considering Pd[22] and vanadia deposits[15] as examples. A corresponding analysis of the STM images in Figure 1 reveals that V-particles are partially incorporated into the alumina film. This points toward a strong interaction between vanadium and alumina, a conclusion which is corroborated by XPS and IR spectroscopy.

Apart from particle dimensions, the question where nucleation occurs is an important aspect of particle growth. First of all, the homogeneous distribution of V-aggregates precludes alumina

(12) Bäumer, M.; Freund, H.-J. *Prog. Surf. Sci.* **1999**, *61*, 127.
(13) Frank, M.; Bäumer, M. *Phys. Chem. Chem. Phys.* **2000**,*2*, 3723.
(14) Copéret, C.; Chabanas, M.; Saint-Arroman, R. P.; Basset,J.-M. *Angew. Chem., Int. Ed.* **2003**, *42*, 156.
(15) Magg, N.; Giorgi, J. B.; Schroeder, T.; Bäumer, M.;Freund, H.-J. *J. Phys. Chem. B* **2002**, *106*, 8756.
(16) Magg, N.; Giorgi, J. B.; Hammoudeh, A.; Schroeder, T.;Bäumer, M.; Freund, H.-J. *J. Phys. Chem. B* **2003**, *107*, 9003.
(17) Magg, N. Ph.D. Thesis, Humboldt Universität, Berlin, 2003(english language).
(18) Hoffmann, F. M. *Surf. Sci. Rep.* **1983**, *3*, 107.
(19) Jaeger, R. M.; Kuhlenbeck, H.; Freund, H.-J.; Wuttig, M.;Hoffmann, W.; Franchy, R.; Ibach, H. *Surf. Sci.* **1991**, *259*, 235.
(20) Stierle, A.; Renner, F.; Streitel, R.; Dosch, H. *Phys. Rev.B* **2001**, *64*, 165413.

(21) Bäumer, M.; Biener, J.; Madix, R. J. *Surf. Sci.* **1999**, *432*,189.
(22) Hansen, K. H.; Worren, T.; Laegsgaard, E.; Besenbacher,F.; Stensgaard, I. *Surf. Sci.* **2001**, *475*, 96.
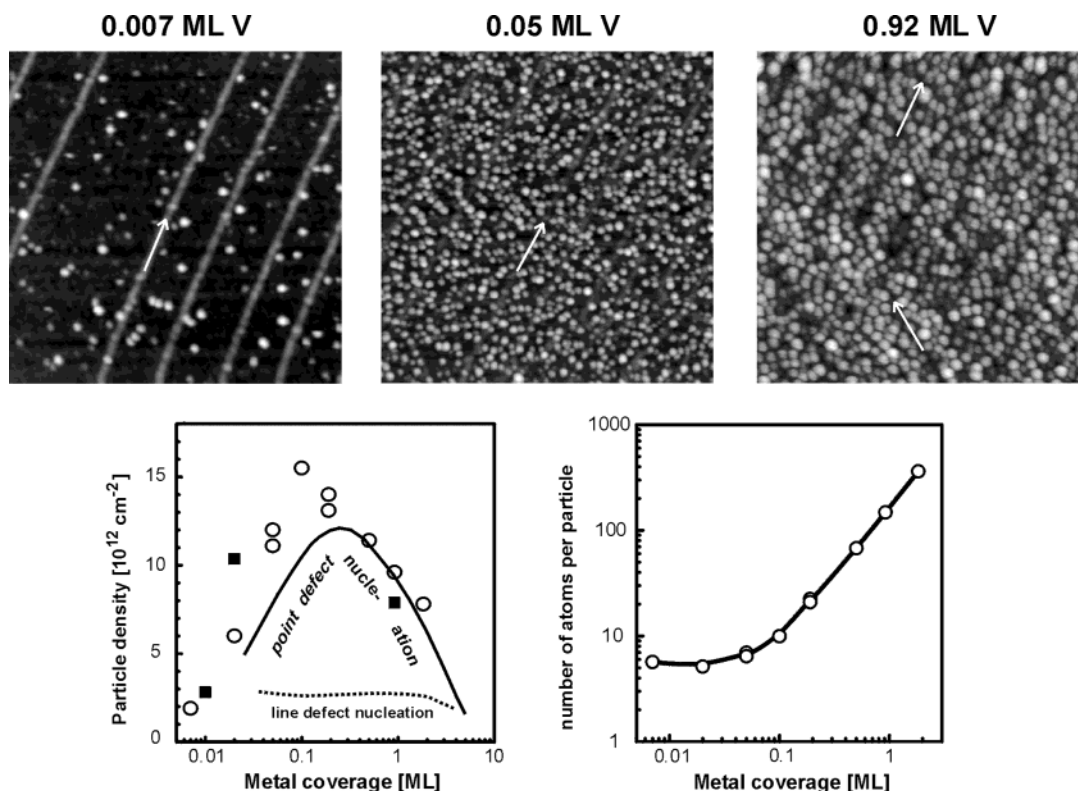
Figure 1. Top: STM images (100 nm × 100 nm, $U = 2.3-3.1$ V, $I = 0.04-0.1$ nA) after vanadium deposition on alumina at 300 K and under UHV conditions. The amount deposited is indicated at the top of each image. The white arrows mark the antiphase domain boundaries of the alumina substrate. Bottom: Vanadium particle number density and number of V-atoms per particle plotted as a function of V-coverage for deposition at 300 K (○) and at 90 K (■). Furthermore, curves are shown which are characteristic for metal nucleation at line and point defects, respectively. They were determined from previous studies on Rh, Pd, Ir, Pt, and Co growth.[12,13]

line defects as dominant nucleation sites. Interestingly, a strong interaction with line defects is noticed at higher V-coverages (e.g., 0.92 MLV), leading to a characteristic network of dark stripes in the STM images. Obviously, a nearly complete incorporation of vanadium into the film has taken place there. Although it is well-known that line defects represent the deepest potential wells on the Al_2O_3 film, nothing comparable has been observed for the noble metals studied so far.

Point defects with a number density of ~1×10^{13} cm^{-2} are a further type of nucleation centers on the alumina film.[13] By counting the number of V-particles in several STM images and averaging the area-normalized values, we determined the number density of V-particles as a function of the metal exposure. This is shown in the lower left corner of Figure 1, together with curves that are characteristic for metal nucleation at point and line defects,[12,13] respectively. Based on this comparison, point defects seem to be the preferred nucleation sites of room-temperature grown vanadium. That the V-data are slightly shifted toward lower metal coverage and higher particle density probably reflects the stronger particle–support interaction present for V/Al_2O_3, inducing a more two-dimensional growth mode.

Deposition at lower sample temperatures is expected to bear a strong influence on the metal nucleation behavior. This was shown for Rh and Pd aggregates, which preferentially decorate alumina line defects at 300 K but nucleate at point defects if metal deposition is performed at 90 K.[12,13] So far, only a few STM images exist for vanadium growth at 90 K which basically look identical to the room-temperature preparations (therefore
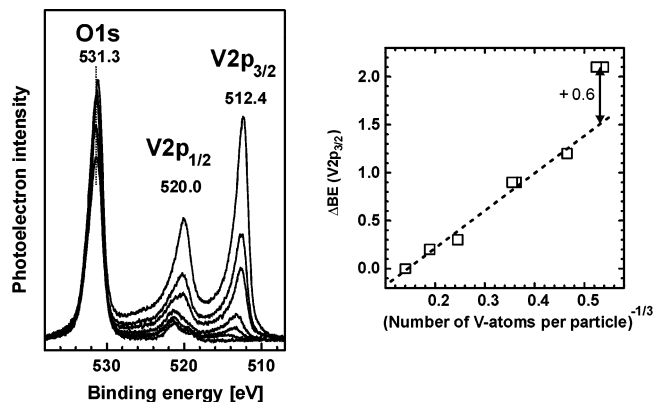
Figure 2. Series of Al Kα excited XP spectra taken for V/Al_2O_3 at different V-loadings (0, 0.05, 0.1, 0.19, 0.5, 0.92, and 1.83 MLV). Right: Illustration of the linear correlation between V2p$_{3/2}$ BE-shifts and (number of V-atoms per particle)$^{-1/3}$, a quantity which is proportional to the reciprocal particle diameter. As indicated, the last data point (0.05 MLV) deviates from this relation by about +0.6 eV.

not shown). Yet, there are interesting differences as revealed by the CO adsorption experiments discussed below.

Because particle diameters determined by STM are not always a reliable measure for their actual sizes (tip convolution effects!), the average number of metal atoms per particle is often more meaningful. This quantity was calculated dividing the number of atoms evaporated onto the surface per cm^2, which is known from the calibration with a quartz microbalance, by the determined particle number density. As evidenced by Figure 1 (lower right corner), vapor deposition allows one to grow

V / Al$_2$O$_3$
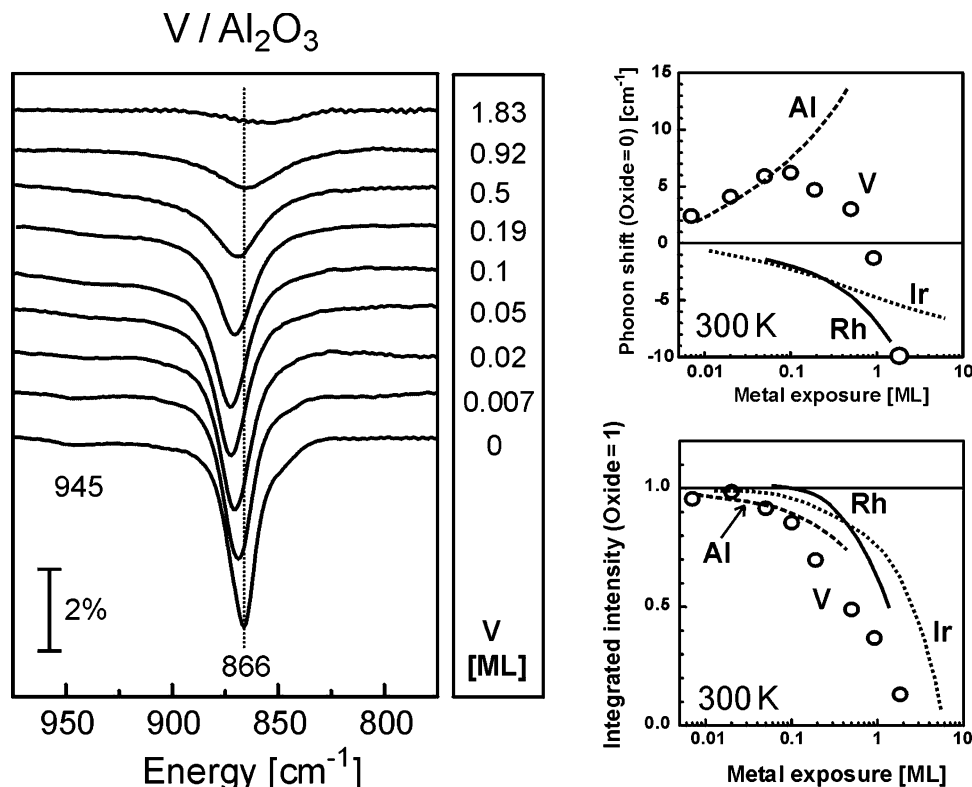
Figure 3. Left: Room-temperature IR spectra taken for increasing V-coverages (see panel on the right side). Spectra are referenced to clean NiAl at 300 K. Right: Behavior of the most prominent alumina phonon at 866 cm^{-1} as a function of metal exposure. Phonon shifts and integrated band intensities are given relative to the clean alumina film. The ○ symbols represent V data points from this work, whereas the lines summarize studies on Al (dashed), Rh (solid), and Ir (dotted) room-temperature deposits performed previously.[25,30]

V-particles with average sizes ranging from a few atoms up to several hundred atoms.

3.1.2. XPS Results. Figure 2 displays XP spectra in the region of O1s and V2p emissions, measured as a function of V-coverage. Considering the decreasing oxygen and the increasing V-signal intensities, the growth of an overlayer on top of the alumina film is obvious. To determine its chemical state, the V2p$_{3/2}$ peak position has to be analyzed (note that the V2p$_{1/2}$ spin−orbit component overlaps with intensity from the O1s peak produced by X-ray satellites). At multilayer amounts of vanadium, we measured a V2p$_{3/2}$ binding energy (BE) of 512.4 eV which corresponds to literature data for metallic vanadium.[23] At lower coverages, this signal is increasingly shifted toward higher BE, suggesting that smaller particles might be oxidized to a certain extent.

Previous electronic structure investigations on alumina thin-film supported metal particles have demonstrated that shifts of this kind might be explained also by particle-size-dependent final state effects.[12,24,25] Such contributions to the binding energy occur because electrons cannot tunnel through the alumina film, on the time scale of the photoemission process. Based on a simple electrostatic model, a linear relationship between BE shifts and the inverse particle diameter is then expected.[26] In Figure 2, the measured V2p$_{3/2}$ binding energies are plotted versus (number of vanadium atoms per particle)$^{-1/3}$, a quantity

which is inversely proportional to the particle diameter. It seems that final state contributions dominate the observed peak shifts.

However, an accurate distinction between initial and final state effects is difficult, in particular for very small particles, where lattice strain, changes in the coordination of the atoms, and interactions with the substrate might play a significant role.[27,28] In fact, the deviation from the linear behavior by about +0.6 eV identified at the lowest coverage in Figure 2 (0.05 MLV) points to the presence of vanadium in an oxidation state close to +1. This is in accordance with recent X-ray absorption (XAS) experiments by Madix et al.,[21] according to which low V-coverages (<0.1 MLV) are oxidized through the contact to alumina (V^{+x}, $1 < x < 2$). Similar conclusions have been drawn for Al/Al$_2$O$_3$/NiAl(110), where band-bending effects were interpreted in terms of a metal-to-oxide transfer of charge.[29]

3.1.3. IRAS Results. Figure 3 presents room-temperature infrared spectra for V-coverages in the range of 0−1.83 MLV. The pristine support is characterized by a series of phonon signals, the most prominent of which is located at 866 cm^{-1}. Upon V-deposition, this feature gets rapidly attenuated and broadened. Concomitantly, changes in its vibration frequency are observed. Up to an exposure of ∼0.1 MLV, the band shifts to higher energies, but thereafter it moves back and eventually attains energy values below that of the pristine oxide. For comparison, integrated phonon intensities and relative phonon shifts are plotted in Figure 3 as a function of V-coverage (○),

(23) Sawatzky, G. A.; Post, D. *Phys. Rev. B* **1979**, *20*, 1546.
(24) Sandell, A.; Libuda, J.; Brühwiler, P. A.; Andersson, S.; Maxwell, A. J.; Bäumer, M.; Mårtensson, N.; Freund, H.-J. *J. Vac. Sci.Technol., A* **1996**, *14*, 1546.
(25) Frank, M. Ph.D. Thesis, Humboldt Universität, Berlin,2000 (german language).
(26) Wertheim, G. K. *Z. Phys. B* **1987**, *66*, 53.

(27) Mason, M. G. *Phys. Rev. B* **1983**, *27*, 748.
(28) Richter, B.; Kuhlenbeck, H.; Freund, H.-J.; Bagus, P. S.*Phys. Rev. Lett.*, submitted.
(29) Libuda, J.; Frank, M.; Sandell, A.; Andersson, S.; Brühwiler, P. A.; Bäumer, M.; Mårtensson, N.; Freund, H.-J. *Surf. Sci.* **1997**,*384*, 106.

together with curves obtained after deposition of Al, Rh, and Ir at 300 K.[25,30] All of these metals induce a qualitatively similar damping behavior, albeit V exerts a somewhat stronger influence. Very surprising are the observed phonon shifts. Within the coverage regime examined, Al causes a substantial blue-shift, whereas Rh and Ir both induce moderate red-shifts. The clear crossover found for V-particles implies that there are at least two factors which govern frequency shifts and whose relative impact depends not only on metal coverage but also on the nature of the deposited metal.

As discussed in detail in refs 25 and 30, there are many conceivable possibilities as to how oxide phonons might be influenced by metal deposits. To distinguish them experimentally, we have studied deposits with different electronic and chemical properties prepared under identical conditions on the same support. In addition, heating and gas adsorption (CO, C_2H_4) experiments have been performed.[25,30]

Briefly, we managed to show that some of the possible mechanisms are only of minor relevance for metal-induced changes of phonon bands: mechanical detuning by the additional mass attached to the system, Pauli repulsion between oxide and metal electrons, as well as electron–phonon scattering. Instead, the fact that clear blue-shifts were caused only by the two most reactive metals (Al, V), both get partially oxidized in the interface region, indicated that chemical interactions are decisive, at least at low coverages. At higher coverages, other mechanisms take over control as demonstrated by the frequency crossover in the V/Al_2O_3 case. In this regime, the extent of metallicity should increasingly influence the dielectric response of the system, either through direct screening or dipole–image dipole interactions.

Support for this idea comes from a series of low-temperature Ir preparations for which a correlation between effective phonon attenuation and efficient metallic screening was found.[25,30] The same experiments revealed, however, that metallic screening capabilities are not necessarily needed to induce phonon shifts. This is in line with recent studies on thin, well-ordered silica films, another model support that can be prepared on the Mo-(112) surface.[31,32] Although vanadium particles deposited onto this support exhibit very similar dimensions, and therefore very similar screening properties such as their alumina-supported counterparts, much larger phonon shifts are observed on silica than on alumina.[17,33] Hence, screening properties play only a minor role for phonon shifts. It seems that the situation is even more complex than originally thought: there are several distinct factors which influence the phonon behavior whose relative impact depends not only on metal coverage but also on the considered phonon property (damping, shift, or broadening).

3.2. CO Adsorption. Following the discussion of structural properties, this section concentrates on the interaction between alumina-supported vanadium and carbon monoxide. Within the three subunits, basic low-temperature adsorption, isotope mixture experiments, and charge-transfer effects at the interface are discussed.

CO / V / Al₂O₃ (300K)

2093
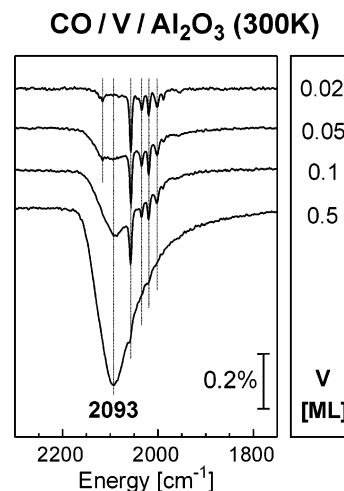
Figure 4. IR spectra from CO-saturated vanadium particles grown on alumina at 300 K. CO adsorption and subsequent spectrum acquisition were carried out at 90 K. The right-hand panel indicates the vanadium loading.

3.2.1. Low-Temperature CO Adsorption. Figure 4 presents IR spectra for room-temperature grown vanadium taken after CO saturation at 90 K. At very low vanadium coverages, the spectra consist of a series of well-separated, narrow peaks with a full width at half-maximum (fwhm) of ~5−7 cm⁻¹. Upon increasing V-loading, there is a gradual transition to a broad absorption band. Its frequency of ~2093 cm⁻¹ is typical for the adsorption of CO on metal surfaces in a terminal geometry.[18,34]

Only a few vibrational studies are available in the literature for CO adsorption on V-surfaces. This is mostly due to the difficulty in preparing single crystalline surfaces with sufficient purity, as several hundred hours of sputtering and annealing are required to remove both oxygen and carbon contaminations.[35] In one study, CO was adsorbed on a V-film grown by deposition of gas-aggregated clusters onto a hydrocarbon oil matrix that was supported by the salt window of an IR-cell. Transmission IR spectroscopy gave rise to a broad band (fwhm ≈ 200 cm⁻¹) consisting of two peaks at 1940 and 1890 cm⁻¹.[36] The presence of hydrocarbons, however, precludes a reliable comparison of this system to our work. Another set of data was published for a vanadium-promoted Rh catalyst.[37] There, a band was observed at 2015 cm⁻¹ which was assigned to CO bound to vanadium. Yet also in this case it is not clear in what chemical state vanadium existed on the surface.

Nonetheless, the asymmetric peak shape and the large peak width of the feature at 2093 cm⁻¹ (fwhm ≈ 100 cm⁻¹ as compared to typical values <50 cm⁻¹ for CO on other alumina-supported metal particles[13,38]) reflect a broad distribution of adsorption sites available on our vanadium particles. This is in line with the strong metal–support interaction identified in the previous sections and points to the growth of small and disordered aggregates.

(30) Frank, M.; Wolter, K.; Magg, N.; Heemeier, M.; Kühnemuth, R.; Bäumer, M.; Freund, H.-J. *Surf. Sci.* **2001**, *492*, 270.
(31) Schroeder, T. Ph.D. Thesis, Humboldt Universität, Berlin,2001 (english language).
(32) Schroeder, T.; Giorgi, J. B.; Bäumer, M.; Freund, H.-J.*Phys. Rev. B* **2002**, *66*, 165422.
(33) Magg, N.; Immaraporn, B.; Giorgi, J. B.; Schroeder, T.;Bäumer, M.; Freund, H.-J., in preparation.

(34) Hayden, B. E. Reflection Absorption Infrared Spectroscopy: Vibrational Spectroscopy of Molecules on Surfaces. In *Methods of Surface Characterization*; Yates, J. T., Madey, T. E., Jr., Eds.; PlenumPress: New York, London, 1987; Vol. 1.
(35) Beutl, M.; Lesnik, J.; Lundgren, E.; Konvicka, C.; Varga,P.; Rendulic, K. D. *Surf. Sci.* **2000**, *447*, 245.
(36) Blyholder, G.; Allen, M. C. *J. Am. Chem. Soc.* **1969**, *91*,3158.
(37) Koerts, T.; Welters, W. J. J.; van Wolput, J. H. M. C.;van Santen, R. A. *Catal. Lett.* **1992**, *16*, 287.
(38) Frank, M.; Kühnemuth, R.; Bäumer, M.; Freund, H.-J.*Surf. Sci.* **1999**, *427−428*, 288.
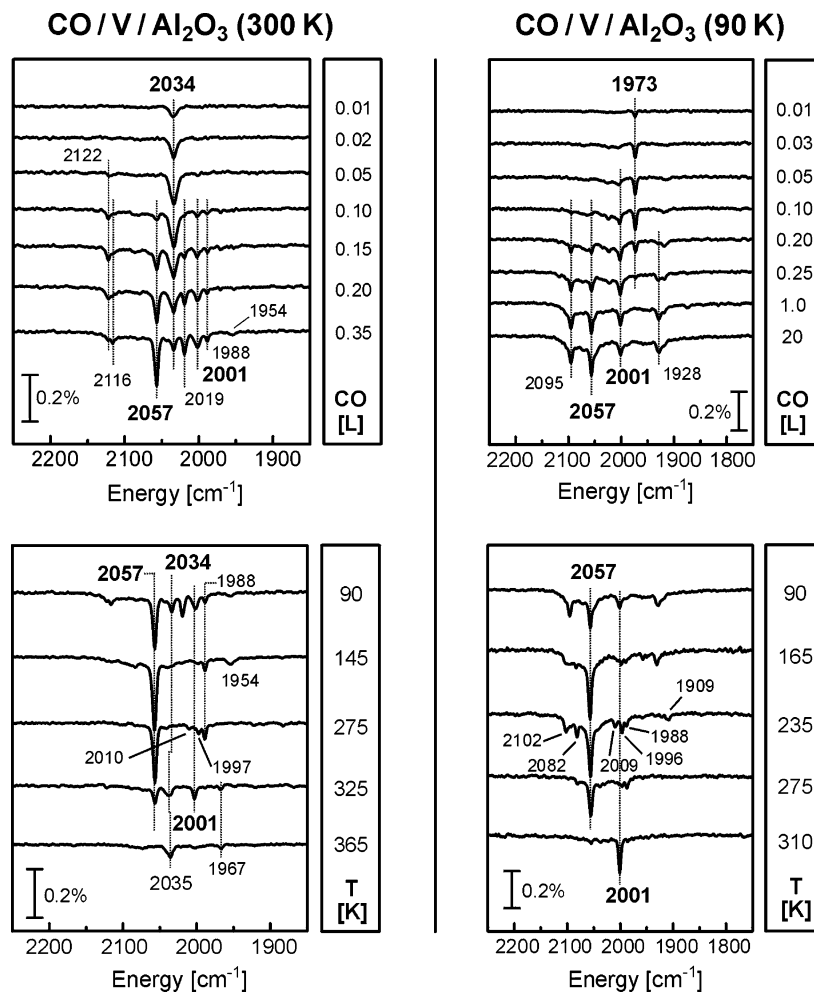
Figure 5. IR spectra taken from alumina-supported vanadium (0.20 MLV) grown at 300 K (left column) and 90 K (right column), respectively. For both preparations, the upper row shows spectra for increasing CO exposure at 90 K, while the lower row presents a heating series performed after CO saturation.

Superimposed onto this broad band, a complex structure of narrow peaks is visible in Figure 4 up to the highest coverage examined where small modulations on the low-energy tail of the broad signal can still be detected. Most notably, their frequency positions are constant throughout the entire spectra series, emphasized by dotted lines in Figure 4. Together with the extremely low peak width, this is reminiscent of isolated $M_x(CO)_y$ metal carbonyl species on technical catalysts.[39,40] Apart from their importance in catalysis, such complexes are often regarded as cornerstones of modern coordination and organometallic chemistry.[41] In addition, they serve as models for the binding of CO to metal surfaces.[18] Spectroscopic investigation of metal carbonyls is often performed via matrix-isolation[42] and gas-phase techniques.[43] Recent experiments in our group have demonstrated that surface metal carbonyls, $M_x(CO)_y$ with M = (Rh, Pd, Ir), can be produced by vapor deposition of metals onto Al_2O_3/NiAl(110) and subsequent adsorption of CO.[44,45] For a successful preparation, it was necessary to deposit these metals

at low temperatures (60−90 K) to generate sufficiently small aggregates. In the case of vanadium, such aggregates are formed already at room temperature, which again reflects the strong interaction between vanadium and alumina. That this behavior is due to the combination of V and Al_2O_3 was discovered in experiments with silica-supported vanadium. On this support oxide, vanadium carbonyls could be generated only via metal deposition at 90 K but not at 300 K (more details will be provided below, in the discussion of Figure 6).

To obtain a deeper understanding of the properties of CO/ V/Al_2O_3, both 300 and 90 K deposits have been studied as a function of CO exposure and sample heating performed after CO saturation. Corresponding spectra and frequency values are given in Figure 5 and Table 1, respectively. The following discussion of these results will start with the room-temperature preparation.

CO Exposure Series (300 K). At very low CO dosages, only a single peak is visible at 2034 cm^{-1}, suggesting that the associated species might consist of only a single CO molecule. That this is true was proven by isotope mixture experiments presented in section 3.2.2. The intensity of this monocarbonyl species grows until a CO exposure of ∼0.1 L. Thereafter, the peak decreases again, while several new features start to appear simultaneously. At saturation, at least eight peaks can be

(39) Diaz, A. L.; Quigley, W. W. C.; Yamamoto, H. D.; Bussell, M. E. *Langmuir* **1994**, *10*, 1461.
(40) Basset, J.-M.; Lefebvre, F.; Santini, C. *Coord. Chem. Rev.* **1998**, *178−180*, 1703.
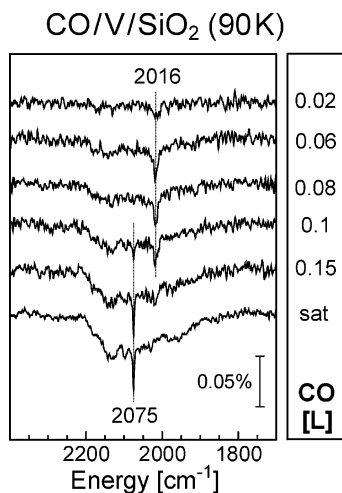(41) Cotton, F. A.; Wilkinson, G.; Murillo, C. A.; Bochmann, M. *Advanced Inorganic Chemistry*, 6th ed.; Wiley: New York, 1999.
(42) Zhou, M.; Andrews, L.; Bauschlicher, C. W., Jr. *Chem. Rev.* **2001**, *101*, 1931.
(43) Weitz, E. *J. Phys. Chem.* **1994**, *98*, 11256.
(44) Frank, M.; Kühnemuth, R.; Bäumer, M.; Freund, H.-J. *Surf. Sci.* **2000**, *454−456*, 968.
(45) Frank, M.; Bäumer, M.; Kühnemuth, R.; Freund, H.-J. *J. Phys. Chem. B* **2001**, *105*, 8569.

CO/V/SiO₂ (90 K)

Figure 6. IR spectra from silica-supported vanadium (0.03 MLV) deposited at 90 K. Spectra were measured for increasing CO exposure at 90 K.

Table 1. Stretching Frequencies [cm⁻¹] Measured after Adsorption of ¹²CO on Vanadium Particles Deposited on Alumina at 300 and 90 K, Respectively[a]

type	V-deposition at 300 K	V-deposition at 90 K	Ne-matrix
VCO	2034	1973	1931
(isotope pattern)	2032, 1988	1973, 1928	1931, 1888
V(CO)₂	2001	2001	1944
(isotope pattern)		2001, 1983, 1955	1944, 1926, 1900
V(CO)₃	2057	2057	1911
(isotope pattern)	2057, 2042, 2028, 2011		1911, −, −, 1869
not assigned	2122	2095	
not assigned	2116	2071	
not assigned	2019	2023	
not assigned	1988	1928	
not assigned	1954	1917	

[a] Corresponding data are provided for Ne-matrix isolated vanadium carbonyls reported in the literature.[42,48] In the cases where an assignment of the carbonyl stoichiometry was possible, additional frequency values are given for experiments with ¹²CO−¹³CO isotope mixtures.

distinguished in the spectrum. They all seem to develop in a unique way, indicating that they belong to different species. It is important to emphasize again that their frequency positions are independent of both CO- and V-coverage.

Heating Series (300 K). The IR spectra in the lower left corner of Figure 5 were measured after heat treatment of CO-saturated 300 K deposits. Heating to 145 K removes most of the species present at saturation. The feature at 2057 cm⁻¹, however, has increased upon heating; that is, at least part of the other species must have been converted into this one. Such a conversion could proceed, in principle, via diffusion and agglomeration of whole $V_x(CO)_y$ entities or via abstraction of CO, according to the scheme $V_x(CO)_y \rightarrow V_x(CO)_{y-1} + CO_{gas}$. The former scenario seems unlikely, at first glance, because V-aggregates should be stable at temperatures below 300 K where they had been prepared. Yet it is conceivable that the formation of a CO complex weakens the metal−support bond (bond-order conservation[46]). A definite statement is possible only if the stoichiometry of the involved species is known. Further heating to 275 and 325 K decreases the 2057 cm⁻¹ feature again, while new peaks appear that have not been observed in the

spectra so far (2010, 1997, and 1967 cm⁻¹). At the highest temperature applied, only one species is left at a frequency close to that of the monocarbonyl position (2034 cm⁻¹).

Finally, there are indications that part of the CO molecules might dissociate upon heating.[17] However, this topic has not been investigated in detail so far and will therefore be addressed in future experiments.

CO Exposure Series (90 K). Adsorption of CO on the 90 K deposits results in a series of narrow carbonyl peaks similar to that in the 300 K case. However, there are also clear differences between these preparations as shown in Figure 5. The mono-carbonyl, for example, which is the first species to appear at very low CO dosages, is located now at a lower frequency (1973 cm⁻¹ as compared to 2034 cm⁻¹). It initially grows upon CO exposure but later on its intensity decreases again and finally even vanishes. Concomitantly, new species start to emerge. At CO saturation, the spectrum is dominated by four peaks, two of which exist also for the 300 K preparations (2057 and 2001 cm⁻¹).

In conclusion, the deposition temperature clearly influences the properties of deposited vanadium particles, although their overall morphology, as probed by STM, seems to be essentially independent of this preparation parameter. Hence, differences in the vanadium−alumina interface region are expected to be at the origin of these findings. That this is really true will be shown in the following sections.

Heating Series (90 K). Again, most species present at saturation disappear quickly, while the peak at 2057 cm⁻¹ grows at their expense. In addition, new features develop. Two of them are close to features observed after heat treatment of the 300 K deposits (2010 and 1997 cm⁻¹). Interestingly, the carbonyl at 2001 cm⁻¹ is the most stable species now as it is the only one left at the highest temperature examined.

As announced above, Figure 6 presents a series of spectra for increasing CO exposure to silica-supported vanadium deposited at 90 K. At the beginning, only a single narrow peak (fwhm ≈ 10 cm⁻¹) is observed at a position of 2016 cm⁻¹. Above 0.08 L, a new peak shows up at 2075 cm⁻¹ (fwhm ≈ 5 cm⁻¹) which seems to develop at the expense of the former one and is the only carbonyl-like species present after CO saturation. In addition, a broad feature appears in the region between 1900 and 2200 cm⁻¹ due to CO adsorbed on irregularly shaped, larger aggregates. The narrow peak at 2016 cm⁻¹ is most likely associated with a VCO monocarbonyl, whereas the signal at 2075 cm⁻¹ should originate from a $V(CO)_y$ species with $y \geq 2$. Based on the intensity development of the two carbonyl peaks, $y = 2$ seems to be a reasonable assumption.

3.2.2. Adsorption of CO Isotope Mixtures. A definite stoichiometric assignment of the vanadium carbonyls prepared requires studies with CO isotope mixtures. Corresponding IR spectra have been measured after adsorption of ¹²CO, ¹³CO, and an equimolar mixture of these isotopes, respectively. This should lead to characteristic frequency and intensity patterns.[47] However, the large number of small and strongly overlapping features present in our case leads to very complex spectra following the adsorption of isotopic mixtures. This precludes an assignment of all $V_x(CO)_y$ species generated. Yet some of them can be prepared in such a way that interference from other signals is negligible, and, in these advantageous cases, isotopic

(46) Shustorovich, E.; Sellers, H. *Surf. Sci. Rep.* **1998**, *31*, 5.

(47) Darling, J. H.; Ogden, J. S. *J. Chem. Soc., Dalton Trans.* **1972**, 2496.
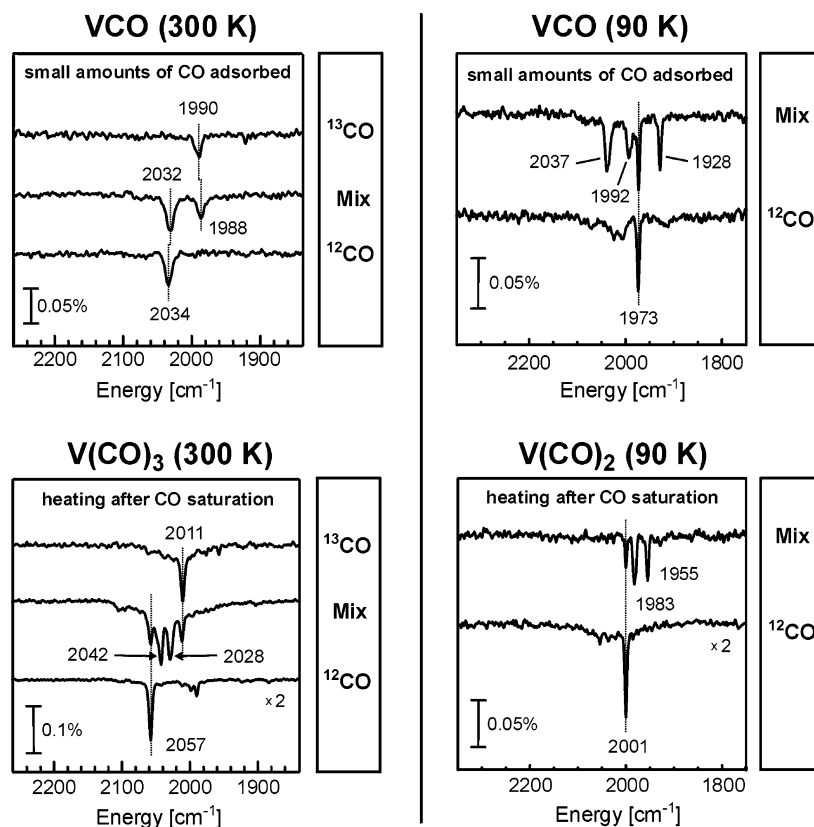
Figure 7. IR spectra from vanadium carbonyls prepared at 300 K (left) and at 90 K (right), respectively. Spectra were taken after adsorption of ^{12}CO, ^{13}CO, and an equimolar mixture of these isotopes (note that for the CO mix experiments presented in the right column, the deposition of V was performed at 120 K; see text for more details). First row: adsorption of small amounts of CO to isolate the initial species in the CO exposure series. Second row: spectra after CO saturation and subsequent heating to 220 K (left) and 310 K (right) to isolate the most stable species.

labeling proved to be a valuable tool. As before, the presentation starts with results for the 300 K deposits.

Monocarbonyl (300 K). As shown in Figure 5, the feature at 2034 cm^{-1} is the only signal present in the spectrum for very low CO exposures. This situation is ideal for isotope mixture experiments. The corresponding spectra in Figure 7 (left) reveal a double-peak structure whose high- and low-energy parts coincide nearly perfectly with the peak positions determined for pure ^{12}CO and ^{13}CO dosages. This is an unambiguous fingerprint for a V_xCO species. According to the literature on matrix-isolation studies,[48] only a single V-atom ($x = 1$) can be involved because monocarbonyl frequencies for divanadium or higher species are well below 1900 cm^{-1}. For the $^{12}CO-^{13}CO$ splitting, we obtained a value of -44 cm^{-1}. This compares well with results from Ne-matrix isolated VCO:[48] 1931 (^{12}CO) and 1888 cm^{-1} (^{13}CO).

Interestingly, the peak positions of alumina-supported VCO are higher by about 100 cm^{-1} as compared to their Ne-matrix counterparts. One might argue that this is due to the different chemical environments encountered. In fact, experiments with different rare-gas matrices have demonstrated the importance of the chemical environment: VCO frequencies increase from 1868 cm^{-1} for Xe to 1904 cm^{-1} for Ar.[49] Ne-matrices represent the least rigid type of rare-gas matrices and lead to frequencies close to the corresponding gas-phase values. Typically, Ne-induced shifts are below 1%, that is, smaller than 20 cm^{-1}.[50]

Hence, matrix effects cannot explain the large frequency shift observed. The fact that CO stretching frequencies in VCO depend on the angle Φ between the V$-$C and C$-$O bonds could be an alternative explanation.[49] Yet recent DFT calculations clearly favor a linear equilibrium geometry both in the gas phase[51,52] and on surfaces.[51] Electron spin resonance (ESR) experiments for VCO in rare-gas matrices favor this structure as well.[53] Finally, CO stretching frequencies in carbonyl complexes depend on the charge state of their metal center, that is, the extent of metal-to-CO π-back-donation.[42] It turns out that such effects indeed play a crucial role for the observed frequency shifts. A more detailed account of this subject will be given in the following section.

For completeness, it shall be mentioned that the intensity ratio between ^{12}CO- and ^{13}CO-monocarbonyls in Figure 7 is not 1:1 as one would expect for an equimolar mixture. Experimental shortcomings, probably a defective leak valve in the gas feed lines, are most likely the source of this deviation.

Tricarbonyl (300 K). According to Figure 5 (lower left corner), the feature at 2057 cm^{-1} can be prepared as an isolated species as well, provided that CO saturation is followed by heating to about 145$-$275 K. Upon adsorption of an isotope mixture, the single ^{12}CO-peak splits into four signals (2057, 2042, 2028, and 2011 cm^{-1}), while exposure to pure ^{13}CO gives rise to a single peak at 2011 cm^{-1} (cf., Figure 7, left). Hence, the low- and high-frequency peaks in the isotope spectrum

(48) Zhou, M.; Andrews, L. *J. Phys. Chem. A* **1999**, *103*, 5259.
(49) Hanlan, L.; Huber, H.; Ozin, G. A. *Inorg. Chem.* **1976**,*15*, 2592.
(50) Jacox, M. E. *Chem. Phys.* **1994**, *189*, 149.

(51) Fournier, R. *J. Chem. Phys.* **1993**, *99*, 1801.
(52) Adamo, C.; Lelj, F. *J. Chem. Phys.* **1995**, *103*, 10605.
(53) Van Zee, R. J.; Bach, S. B. H.; Weltner, W., Jr. *J. Phys.Chem.* **1986**, *90*, 583.

originate from the pure species, whereas the other two contain both isotopes. Such a frequency pattern is typical for a $V_x(CO)_3$ tricarbonyl. Ne-matrix studies identified a $V(CO)_3$ carbonyl at 1911 cm^{-1}, thus favoring again a species with $x = 1$.[48]

Considering the structure of our $V(CO)_3$ species, a planar geometry can be excluded on the basis of the metal surface selection rule (MSSR). DFT calculations[48] predict a pyramidal structure with C_{3v} symmetry and a symmetric A_1-mode with a dynamic dipole moment perpendicular to the substrate surface. In addition, there should be an asymmetric E-mode with an intensity higher than that of the A_1-mode. As it is not observed in our spectra, we conclude that its dynamic dipole is oriented essentially parallel to the substrate.

The comparison with previous studies on $V(CO)_3$ is complicated insofar as there is considerable disagreement between matrix-isolation[48,49] and gas-phase[54] experiments with respect to its structure and hence its IR modes. However, our frequency pattern compares well with other literature reports on $M(CO)_3$ carbonyls of C_{3v} symmetry. The A_1-mode of $Sc(CO)_3$, for example, produces a four-peak structure with very similar peak separations of -13, -14, and -17 cm^{-1}.[55]

Again, the measured intensity pattern of about 1:2:2:1 is not compatible with statistical abundances, assuming exposure to an equimolar CO mixture (1:3:3:1). In part, this might be due to the difficulty of assigning a proper baseline because the carbonyl peaks overlap with the broad CO signal from larger vanadium particles. In addition, the above-mentioned experimental shortcomings make it impossible to determine the ^{12}CO/^{13}CO ratio actually adsorbed. The frequency pattern is therefore a more reliable indicator, and one should ask if there are other carbonyl stoichiometries which could lead to a four-peak pattern as well. First of all, $V(CO)_y$ species with $y \geq 4$ can be ruled out. Their isotope spectra would consist of more than four peaks.[47] The only conceivable alternative is a special type of dicarbonyl for which the gas-phase C_{2v} symmetry is reduced to the C_s point group through interactions with the support. Such a scenario is rather unlikely; besides, it would lead to a 1:1:1:1 intensity pattern that is not observed either. Hence, the species at 2057 cm^{-1} is assigned to a tricarbonyl.

Dicarbonyl (90 K). Further insight into carbonyl stoichiometries comes from low-temperature preparations. According to Figure 5 (lower right corner), heating ^{12}CO-saturated particles to ∼310 K allows one to isolate a species at 2001 cm^{-1}. Repeating this procedure with a CO mixture leads to a three-peak structure with signals at 2001, 1983, and 1955 cm^{-1} (Figure 7, right). The splitting pattern is in good agreement with matrix-isolation data for the symmetric A_1-mode of a bent $V(CO)_2$ species.[48] Note that the dicarbonyl that we have generated must exhibit a bent structure because the MSS rule would preclude the detection of a linear species. For both geometries, the associated asymmetric B_2-mode is screened by metal electrons of the substrate. As before, the measured intensity pattern (1:3:2) differs significantly from the expected one (1:2:1), suggesting that the actual CO mixture was nonequimolar. In general, a ^{12}CO/^{13}CO ratio of $1/\kappa$ results in statistical abundancies of $1:2\kappa:\kappa^2$.[47] Hence, a ^{12}CO/^{13}CO ratio of $1:\sqrt{2}$ would explain our findings.

Monocarbonyl (90 K). One of the most interesting aspects of the 90 K preparations was the observation of a species at 1973 cm^{-1} whose development as a function of CO exposure was very similar to that of the room-temperature grown monocarbonyl at 2034 cm^{-1} (cf., Figure 5, top row). Yet why should VCO prepared at 300 K have a different CO stretching frequency than VCO prepared at 90 K? There are two fundamentally different explanations, both of which rely on differences in the vanadium charge state as this was shown to be the decisive factor determining frequency shifts of monocarbonyls:

(a) Both types of monocarbonyls are located at different alumina support sites. This is conceivable because atom diffusion lengths sensitively depend on the sample temperature. In this case, the extent of charge transfer must depend on the VCO nucleation site.

(b) Both types of monocarbonyls are located at the same alumina support sites. Differences in the VCO charge state might then occur if the underlying charge transfer between metal center and oxide support is a thermally activated process which is more efficient at 300 than at 90 K.

Which of these two explanations actually applies in the present case was discovered in an experiment where vanadium was deposited onto the alumina support at 120 K. Figure 7 (right) compares spectra for a low ^{12}CO dosage onto 90 K deposits and for a low dosage of a CO mixture onto these 120 K deposits. Obviously, the peak at 1973 cm^{-1} splits into two signals with a frequency separation of 45 cm^{-1}. This is clear evidence for a monocarbonyl species. Surprisingly, the spectra contain another pair of signals at 2037 and 1992 cm^{-1} for which no counterpart exists in the ^{12}CO spectrum. Comparison to room-temperature grown VCO (2032 and 1988 cm^{-1}) reveals a close resemblance. These findings rule out point b as a possible explanation for the existence of two different monocarbonyls because both species were prepared now at the same temperature of 120 K.[56] In contrast, point a is compatible with all findings, indicating that the diffusion length of vanadium atoms at 120 K is large enough for some of them to reach the nucleation sites preferentially decorated at room temperature, that is, alumina point defects.

In conclusion, the most important vanadium carbonyl species prepared on the alumina support could be identified via isotope mixture experiments as mono-, di-, and tricarbonyls. The presence of two different kinds of monocarbonyls was found to be correlated with a temperature-dependent nucleation behavior of vanadium on the alumina support. Interestingly, no low-temperature specific di- and tricarbonyls could be detected, just the same species as in the 300 K preparations. It seems that single vanadium atoms get mobile upon adsorption of more than one CO molecule so that they are able to diffuse to sites with a deeper potential well such as the point defects. That mechanisms of this kind indeed play a role was evidenced by Figure 5 (lower left corner): heating 300 K deposits results in

(54) Ishikawa, Y.; Hackett, P. A.; Rayner, D. M. *J. Am. Chem.Soc.* **1987**, *109*, 6644.
(55) Zhou, M.; Andrews, L. *J. Phys. Chem. A* **1999**, *103*, 2964.

(56) One might argue that we are dealing with a two-level system (level 1, weakly oxidized V; level 2, more strongly oxidized V) with a certain transition temperature. If then, by accident, the preparation temperature of 120 K is close to this transition temperature, part of the V-atoms might still be in level 1, while the other part is already in level 2, leading to the observed two VCO species. However, because the exposure to CO was carried out about one-half of an hour after V-deposition at 120 K, this transition from level 1 to level 2 would proceed extremely slowly. We therefore disregard such a mechanism as an explanation for our results.

Table 2. CO Stretching Frequencies [cm^{-1}] for Neutral and Singly Charged Vanadium Monocarbonyls in Ne- and Ar-Matrices[42]

type	Ne-matrix	Ar-matrix
VCO$^+$	2143[a]	2116
VCO	1931	1904
VCO$^-$	1807	

[a] The Ne-matrix value for VCO$^+$ was calculated assuming a similar argon-to-neon blue-shift for VCO$^+$ as for VCO. See text for more details.

Table 3. Charge State in Elementary Units (e) for Neutral and Singly Charged Vanadium Monocarbonyls According to ab Initio Calculations[52,59,60]

type	V charge state	Ni charge state	Pd charge state
MCO$^+$	+0.87	+0.91	+0.83
MCO	+0.125	+0.1	+0.07
MCO$^-$	ca. −0.5[a]	−0.46	−0.46

[a] The charge state for VCO$^-$ was estimated on the basis of a comparison to Ni and Pd monocarbonyls.[61] See text for more details.

the formation of new species, although the preparation temperature was not exceeded.

Apart from the four species discussed above, there are many more signals visible in our spectra whose identity could not be revealed either due to their low intensity in the CO mix spectra or due to a strong overlap with other features. They could belong to higher carbonyls such as tetra-, penta-, and hexacarbonyls, which were successfully identified in matrix-isolation[48,49] and gas-phase[54] experiments, or even larger species such as V$_2$-(CO)$_{12}$.[57] One cannot expect, however, that these species can be prepared on solid surfaces in their preferred, three-dimensional geometry. Alternatively, carbonyls with the same stoichiometry as the ones identified might exist but are located at minority nucleation sites (line defects or step edges).

3.2.3. Charge Transfer at the Interface. The frequencies of the V(CO)$_y$ species observed in this work are substantially blue-shifted as compared to corresponding matrix-isolation studies. This is in line with previous experiments performed in our group with alumina-supported Rh, Pd, and Ir carbonyls.[45] The main reason for these frequency shifts are charge-transfer processes between the metal centers and the oxide support which modify the extent of metal-to-CO π-back-donation.[45] As pointed out by Andrews et al.,[42] this correlation can be used as a measure for the charge state of metal carbonyls. One has to take into account, however, that only part of the charge is localized on the metal center.[58] It is therefore necessary to correct for the difference between the charge state of the carbonyl as a whole and that of the metal center, to establish a proper charge−frequency correlation. In the cases investigated so far, an almost linear charge−frequency relation has been found.

Tables 2 and 3 summarize the relevant data for the VCO system. Because Ne-matrix values are closest to gas-phase results, corresponding data shall be used here to establish a charge−frequency relation for vanadium monocarbonyls. Unfortunately, the data set available in the literature is incomplete, but it is possible to estimate the missing values with reasonable accuracy.

VCO$^+$ Frequency. No Ne-matrix frequencies have been reported for the VCO cation. Andrews et al. suggested that the

associated signal is masked in the IR spectra by strong absorptions due to co-condensed CO molecules trapped inside the Ne-matrix.[42] One therefore would expect a VCO$^+$ frequency in the range of 2140 ± 10 cm^{-1} which is typical for isolated CO in a Ne-matrix.[42] To corroborate this hypothesis, we estimated the frequency of VCO$^+$, assuming that the argon-to-neon blue-shift of +27 cm^{-1} for neutral VCO[42] applies also for the VCO cation. The resulting value of 2143 cm^{-1} indeed falls into the expected regime; that is, we consider our estimation reliable. One should note, however, that the extent of argon-to-neon shift is not necessarily independent of the charge state of the monocarbonyl, as observed, for example, in the case of FeCO.[62]

VCO$^-$ Charge State. So far, no calculations have been published on Mulliken charge distributions for VCO$^-$. Complete data sets can be found for mid-to-late transition metals such as Co, Rh, Ir[63] and Ni, Pd, Pt.[61] Table 3 reveals that Ni and Pd monocarbonyls exhibit similar charge states as the VCO system, at least regarding neutral and cationic species. It seems reasonable therefore to assume that this applies also for the anion carbonyls. This approach is justified by the fact that the resulting charge state for VCO$^-$ of about −0.5 e fits quite well into the expected linear correlation between charge and frequency.

On the basis of this linear relationship, the charge states of the two different types of VCO species at 2034 and 1973 cm^{-1} were determined. Accordingly, vanadium deposition at 300 K leads to V-centers charged by about +0.5 e, whereas 0.2 e are transferred to the oxide in the case of the 90 K preparation. Despite the uncertainties regarding the absolute values, the following conclusions can certainly be drawn from our analysis:

(i) The interaction between single vanadium atoms and the alumina film leads to a charge transfer from the metal to the oxide. This is in accordance with the XPS and XAS results discussed in section 3.1.2.

(ii) The extent of charge transfer depends on the metal nucleation site. It is larger if the metal atoms sit on point defects (300 K preparation) as compared to the case of nucleation at (presumably) regular lattice sites (90 K preparation).[64] DFT calculations for metal atoms on regular terrace sites indeed predict a metal-to-oxide charge transfer.[10,11] However, the situation can be completely different for metal atoms that are bonded to point defects such as oxygen vacancies. Their properties crucially depend on the charge state of the vacancy. Singly charged (F$^+$) or neutral (F) color centers, for example, are expected to show the opposite trend, that is, charge transfer from the oxide to the metal.[65−68]

(iii) The extent of charge transfer depends on the reactivity of the metal toward oxygen. Rh monocarbonyls prepared on the alumina support at 90 K have been shown to nucleate at

(57) Ford, T. A.; Huber, H.; Klotzbücher, W.; Kündig, E. P.; Moskovits, M.; Ozin, G. A. *Inorg. Chem.* **1976**, *15*, 1666.
(58) Zhou, M.; Andrews, L. *J. Am. Chem. Soc.* **1999**, *121*, 9171.
(59) Barnes, L. A.; Bauschlicher, C. W., Jr. *J. Chem. Phys.* **1989**, *91*, 314.
(60) Barnes, L. A.; Rosi, M.; Bauschlicher, C. W., Jr. *J. Chem. Phys.* **1990**, *93*, 609.
(61) Liang, B.; Zhou, M.; Andrews, L. *J. Phys. Chem. A* **2000**, *104*, 3905.
(62) Zhou, M.; Andrews, L. *J. Chem. Phys.* **1999**, *110*, 10370.
(63) Zhou, M.; Andrews, L. *J. Phys. Chem. A* **1999**, *103*, 7773.
(64) Similar observations were made for Ir monocarbonyls, although a considerably smaller frequency difference of ∼19 cm^{-1} was found between IrCO sitting on point defects and on regular lattice sites.[45] Corresponding experiments with RhCO were less conclusive in this respect.[45]
(65) Abbet, S.; Riedo, E.; Brune, H.; Heiz, U.; Ferrari, A. M.; Giordano, L.; Pacchioni, G. *J. Am. Chem. Soc.* **2001**, *123*, 6172.
(66) Bogicevic, A.; Jennison, D. R. *Surf. Sci.* **2002**, *515*, L481.
(67) Abbet, S.; Ferrari, A. M.; Giordano, L.; Pacchioni, G.; Häkkinen, H.; Landman, U.; Heiz, U. *Surf. Sci.* **2002**, *514*, 249.
(68) Heiz, U.; Schneider, W.-D. *J. Phys. D* **2000**, *33*, R85.

point defects. Yet in contrast to the clear charge transfer observed for VCO (300 K), RhCO exhibits an almost neutral charge state.[45]

Note that a similar kind of analysis could, in principle, be performed also for the di- and tricarbonyl species. However, their stretching frequencies depend not only on the charge state of the vanadium center but also on the C–V–C bond angles.[58,63] The only definite knowledge that we have from our IR spectra is that the species are certainly not linear or planar (MSSR). A reliable estimation of the charge transfer is therefore not feasible.

4. Summary and Conclusion

STM, XPS, and IR spectroscopy have been employed to characterize vanadium particles deposited onto a thin-film alumina support under UHV conditions and at temperatures between 90 and 300 K. This kind of preparation leads to the growth of roundish, three-dimensional particles with diameters in the range of 20–40 Å. As evidenced by all three techniques, the vanadium–alumina system is governed by a fairly strong overlayer–support interaction. This becomes most obvious at very small vanadium coverages (<0.1 MLV) where the aggregates are partially incorporated into the alumina film and exhibit an average oxidation state between +1 and +2. Only at higher V-coverages does metallic behavior predominate.

Strong interactions in the V–Al₂O₃ interface region manifest themselves also in a quite complex behavior of the alumina phonons as a function of vanadium exposure. Along with earlier IR investigations on similarly prepared Rh, Pd, Ir, and Al particles, it was possible to classify the importance of potential interaction mechanisms in the dependence of the vanadium coverage. Below ∼0.1 MLV, the tendency of the metal toward oxide formation is the decisive factor. At higher coverages, following coalescence, the extent of metallicity gets increasingly important. Further information can be gained from a comparison of identically prepared particles deposited on a chemically different oxide. Preliminary experiments indicate that silica films grown on Mo(112) represent a promising support system in this respect.[17,33]

Low-temperature CO exposure revealed that larger vanadium aggregates exhibit a broad distribution of adsorption sites, that is, disordered particle structures. Uniform and isolated vanadium carbonyls can be prepared via deposition of very small amounts of vanadium. From the large number of carbonyl species present in our IR spectra, we managed to identify, via CO isotope mixture experiments, the three most important ones as mono-, di-, and tricarbonyls of the V(CO)$_y$ type. Growth studies at 90 and 300 K rendered two kinds of VCO species with different CO stretching frequencies. Most likely, differences in the vanadium nucleation site are responsible for this finding. Based on a comparison to Ne-matrix isolation studies, a charge–frequency relationship was set up, according to which the vanadium metal center is charged by about +0.5 e if VCO sits on alumina point defects, while only 0.2 e are transferred to the oxide in the case where the vanadium center is localized between point defects, presumably at regular lattice sites.